An Isotope-Edited FTIR Investigation of the Role of Ser-L223 in Binding Quinone (Q_B) and Semiquinone (Q_B^-) in the Reaction Center from *Rhodobacter sphaeroides*†

Eliane Nabedryk,*,‡ Mark L. Paddock,§ Melvin Y. Okamura,§ and Jacques Breton‡

Service de Bioénergétique, CEA-Saclay, 91191 Gif-sur-Yvette Cedex, France, and Department of Physics 0319, University of California San Diego, La Jolla, California 92093

Received July 11, 2005; Revised Manuscript Received September 7, 2005

ABSTRACT: In the photosynthetic reaction center (RC) from the purple bacterium *Rhodobacter sphaeroides*, proton-coupled electron-transfer reactions occur at the secondary quinone (Q_B) site. Several nearby residues are important for both binding and redox chemistry involved in the light-induced conversion from Q_B to quinol Q_BH_2. Ser-L223 is one of the functionally important residues located near Q_B. To obtain information on the interaction between Ser-L223 and Q_B and Q_B^-, isotope-edited Q_B^-/Q_B FTIR difference spectra were measured in a mutant RC in which Ser-L223 is replaced with Ala and compared to the native RC. The isotope-edited IR fingerprint spectra for the C═O (C$\underline{\cdots}$O) and C═C (C$\underline{\cdots}$C) modes of Q_B (Q_B^-) in the mutant are essentially the same as those of the native RC. These findings indicate that highly equivalent interactions of Q_B and Q_B^- with the protein occur in both native and mutant RCs. The simplest explanation of these results is that Ser-L223 is not hydrogen bonded to Q_B or Q_B^- but presumably forms a hydrogen bond to a nearby acid group, preferentially Asp-L213. The rotation of the Ser OH proton from Asp-L213 to Q_B^- is expected to be an important step in the proton transfer to the reduced quinone. In addition, the reduced quinone remains firmly bound, indicating that other *distinct* hydrogen bonds are more important for stabilizing Q_B^-. Implications on the design features of the Q_B binding site are discussed.

In the reaction center (RC)[1] from photosynthetic purple bacteria, photochemical energy conversion occurs through coupled electron−proton transfer to a buried quinone molecule Q_B. Light-induced electron transfer is initiated from the primary electron donor P (a dimer of bacteriochlorophyll) through a series of electron acceptors to the primary quinone (Q_A), and then to the secondary loosely bound quinone Q_B. A second electron transfer coupled with the uptake of two protons from the solution results in the formation of the quinol Q_BH_2 that is subsequently released from the Q_B binding site and replaced by another quinone from the pool (*1*). This two-step reaction occurs with observed rate constants $k_{AB}^{(1)}$ for the first electron transfer and $k_{AB}^{(2)}$ for the second electron transfer (eqs 1 and 2),

$$(Q_A^-Q_B) \xrightarrow[k_C]{k_{AB}^{(1)}} (Q_A^-Q_B)^* \xrightarrow{k_{et(1)}} (Q_AQ_B^-) \qquad (1)$$

where k_C is the rate constant of the conformational gate which is the rate-limiting step of the reaction (*2*), $k_{et(1)}$ is the intrinsic electron-transfer rate constant, and $(Q_A^-Q_B)^*$ is the intermediate, and

$$Q_A^-Q_B^- + H^+ \underset{}{\overset{k_{H^+}}{\rightleftharpoons}} Q_A^-Q_BH \xrightarrow[k_{et(2)}]{k_{AB}^{(2)}} Q_AQ_BH^- \qquad (2)$$

where k_{H^+} is the proton-transfer rate constant and $k_{et(2)}$ is the intrinsic electron-transfer rate constant for the second electron transfer which is the rate-limiting step for this reaction (*3*). Interactions between the quinone and the protein facilitate its properties to allow efficient reduction (eqs 1 and 2). The interactions are important for the binding of quinone Q_B, stabilization of the reduced radical Q_B^-, and further proton transfer required for the reduction of Q_B to Q_BH_2.

In the *Rhodobacter* (*Rb.*) *sphaeroides* RC, the Q_B binding pocket is formed by a cluster of polar and acid residues (and water molecules) including Ser-L223, Asp-L213, Asp-L210, Asp-M17, Glu-H173, and Glu-L212 (*4, 5*). Previous results have shown that several of these amino acid residues are important for the proton-transfer processes. These include Ser-L223, Glu-L212, and Asp-L213, located near Q_B (Figure 1), and also several other carboxylic acids located between the Q_B site and the surface (for reviews see refs *1*, *6*, *7*). In addition to interactions with side chains, Q_B and Q_B^- form several possible hydrogen bonds to the backbone at L224 and/or L225 (*4*). These hydrogen bonds can play important roles for binding and stabilization of charged intermediate states (*8*−*10*). They may also be important for establishing

† This work was supported by a NIH grant (GM 41637) to M.Y.O.

* To whom correspondence should be addressed. Mailing address: SBE, CEA-Saclay, Bât. 532, 91191 Gif-sur-Yvette Cedex, France. Phone: 331 69 08 71 12. Fax: 331 69 08 87 17. E-mail: eliane.nabedryk@cea.fr.

‡ Service de Bioénergétique, CEA-Saclay.

§ Department of Physics, University of California San Diego.

[1] Abbreviations: RC, reaction center; Q_B, secondary quinone acceptor; Q_A, primary quinone acceptor; Q_n, ubiquinone-*n*, 2,3-dimethoxy-5-methyl-6-polyprenyl-1,4-benzoquinone; P, primary electron donor; H_A, bacteriopheophytin electron acceptor; FTIR, Fourier transform infrared; *Rb.*, *Rhodobacter*; *Bl.*, *Blastochloris*.

10.1021/bi051328d CCC: $30.25
Published on Web 10/14/2005

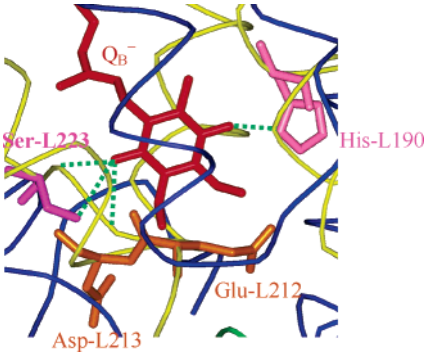

FIGURE 1: Structure of the Q_B^- binding region showing the backbone with Q_B^- (red) and Ser-L223, His-L190 (magenta), and Asp-L213 and Glu-L212 (orange). The C_1 carbonyl group near Ser-L223 forms three hydrogen bonds as indicated by green dashed lines (ref *4*).

the free energy of intermediate states, such as has been proposed for $(Q_A^- Q_B)$* in eq 1 (*9*). Early studies had shown that mutation of Ser-L223 inhibits the turnover of Q_B (*11*, *12*) as well as the binding of competitive inhibitors (*13*, *14*). Here we performed experiments designed to experimentally determine the importance of Ser-L223 on the vibrational properties of the Q_B and Q_B^- states using FTIR difference spectroscopy.

The first RC X-ray structure of *Blastochloris (Bl.) viridis* showed that Ser-L223 was located near the Q_B binding site (*15*), which has been found to be the same in X-ray structures of *Rb. sphaeroides* (*16*−*18*). The availability of higher resolution structures has allowed for more detailed investigations on the interactions between Q_B and the protein. The most controversial issue is the binding position of neutral Q_B. Several different Q_B binding sites have been found in RC crystal structures, and, consequently, large variations in the hydrogen-bonding partner(s) of Ser-L223 have been reported. Ermler et al. (*19*) were the first to describe a different position of Q_B in the RC from *Rb. sphaeroides* (at 2.65 Å resolution) with Q_B displaced by ∼5 Å and occupying a position referred to as the distal site (furthest from Q_A) with only one carbonyl able to interact with the protein (NH of Ile-L224 and C═O of Tyr-L222). In this distal site, no contact with Ser-L223 was possible; however, Q_B was presumed to be in the ubiquinol (Q_BH_2) state. In the Y-strain structure of *Rb. sphaeroides* RCs (*20*), although Q_B occupies a proximal position, Ser-L223 hydroxyl has a different orientation and interacts with Asp-L213. Note that, in *Bl. viridis* RCs, Ser-L223 was originally assigned to form a hydrogen bond to a carbonyl of Q_B (*15*), while in refined structures Ser hydroxyl donates a hydrogen bond to the side chain of Asn-L213 (*21*). In native RCs from *Rb. sphaeroides* exposed to X-rays at cryogenic temperatures (*4*, *22*), two distinct Q_B binding sites, and thus two distinct hydrogen-bonding patterns for Q_B, have been described. In the structure of RCs frozen in the light-adapted state, the quinone was bound preferentially in the proximal site and the C_1 carbonyl of Q_B^- was involved in three branched hydrogen bonds (Figure 1) including the peptide NH groups of Ile-L224 (3 Å) and Gly-L225 (3.3 Å) and the hydroxyl group of Ser-L223 (3.2 Å), with possible weaker interaction with the two latter groups. The second quinone carbonyl interacts with His-L190 (Figure 1). In the dark-adapted structure, the majority of Q_B (≥55%) was bound in the distal site with only one carbonyl of the ubiquinone in polar interaction with the peptide NH of Ile-L224. In the single Ala-M260→Trp mutant RC from *Rb. sphaeroides*, in which Q_A is absent (*23*), the occupancy of the Q_B proximal site with ubiquinone was high and structural details (at room temperature) on the interactions of Q_B were clearly defined with two possible hydrogen bonds between the C_1 carbonyl of Q_B and the backbone amides of Ile-L224 (3.0 Å) and Gly-L225 (3.2 Å) and a third slightly shorter interaction with the Ser-L223 side chain (2.7 Å). In contrast, the crystal structure at 100 K of a quintuple mutant which includes the Ala-M260→Trp mutation showed Q_B at the distal position (*24*) with only one possible hydrogen bond. Note that Pokkuluri et al. (*25*) have observed that the secondary quinone binding position is influenced by temperature and cryoprotectant. Indeed, these authors have found that Q_B occupies the proximal site in native RC samples frozen under dark-adapted conditions (*25*). Thus, there is no consensus as to the preferred binding position of neutral Q_B, and it is not clear what structural role if any Ser-L223 plays in binding the neutral Q_B. On the other hand, there is a consensus on the location of Q_B^-, which places the semiquinone at a location proximal to the non-heme Fe^{2+} and at the approximate symmetry related position of Q_A (*4*, *22*). The hydroxyl side chain of Ser-L223 is in the vicinity (∼3 Å) of the C_1 carbonyl of Q_B^- and therefore could form a hydrogen bond, which has been experimentally observed at low temperatures (77 K) using ENDOR spectroscopy (*26*, *27*). Thus, the functional importance of Ser-L223 can be explained by fast proton transfer through a (transiently formed) hydrogen bond between Ser-L223 and Q_B^-. This model explains the decreased rate of proton-coupled electron transfer (eq 2) in RCs with Ser-L223 replaced with Ala in *Rb. sphaeroides* and *Bl. viridis* (*11*, *12*, *14*, *28*).

The interaction between Ser-L223 and Q_B^- has also been investigated using electrostatic computations made on the crystal structures (*8*−*10*). The calculations show that Ser-L223 can be a hydrogen bond donor to either Q_B (Q_B^-) or the nearby Asp-L213. Earlier calculations by Alexov and Gunner (*8*) already favored an interaction between Ser-L223 and the semiquinone Q_B^-. Recent electrostatic calculations of the midpoint potential of Q_A and Q_B further support that reduction of Q_B requires reorientation of Ser-L223 leading to the formation of a hydrogen bond with Q_B^- (*10*). Notably, the calculations show that the Ser hydroxyl orientation depends on the charge of Asp-L213. If Asp-L213 is ionized when Q_B is neutral, the side chain of Ser-L223 is found to point toward the Asp side chain, away from Q_B. When Asp-L213 is protonated, Ser-L223 donates a proton to Q_B with 80% probability. In both cases, Ser-L223 is a hydrogen bond donor to the semiquinone Q_B^-. Note that protonation of Asp-L213 upon electron transfer to Q_B is not supported by FTIR results on Q_B photoreduction in native RCs and several mutants at the L213 site (*29*, *30*). In addition, molecular dynamics simulations of the Q_A^- to Q_B electron transfer indicate a faster time constant for the reaction when a hydrogen bond is present between Ser-L223 and Q_B^- (*9*). Similar computations for the Ser-L223→Ala mutant RC suggest that a hydrogen bond between Ser-L223 and the quinone is not necessary for the electron-transfer process from Q_A^- to Q_B to occur but may play a crucial role in the reaction kinetics of eq 1 (*9*). However, kinetic measurements

performed in the Ser-L223→Ala mutant RC do not show a significant decrease in the rate of reaction for eq 1 (*11*, *12*). An experimental measure of the interaction energy (hydrogen bond strength) is necessary for solving this issue.

Isotope-edited FTIR difference spectroscopy provides a way to determine the bonding interactions of Q_B and Q_B^- with the protein in RCs. IR difference spectroscopy is an extremely sensitive method for investigating atomic interactions at the level of individual bonds. In particular, the IR frequency of carbonyl bonds is strongly influenced by the surrounding environment (electrostatics and polar interactions). Precise IR fingerprints of the interactions of Q_B before and after photoreduction have been obtained for wild-type RCs from *Rb. sphaeroides* and *Bl. viridis* RCs (*31*−*33*) as well as for a series of mutant RCs (*34*−*36*), using RCs reconstituted with site-specific ^{13}C-labeled ubiquinone. The molecular vibrations of Q_B and Q_B^- can be specifically revealed by calculating double-difference spectra between the Q_B^-/Q_B spectra recorded with ^{13}C-labeled and unlabeled ubiquinone. For both *Rb. sphaeroides* and *Bl. viridis* RCs, the IR fingerprint spectra for $^{13}C_1$ and $^{13}C_4$ labels show a unique C═O band for neutral Q_B at 1641 cm^{-1}, indicative of symmetrical hydrogen bonding of Q_B to the binding site (*31*). Thus, the two carbonyls of Q_B interact with the protein, as it is described in the various X-ray structures of native and mutant RCs when Q_B occupies the proximal site. In wild-type *Rb. sphaeroides* RCs, the IR fingerprint of the semiquinone Q_B^- shows a main band at 1479 cm^{-1} which is similarly shifted by either $^{13}C_1$ or $^{13}C_4$ labels (*31*), thus also favoring symmetrical interactions of the two carbonyls of Q_B^- with the protein.

To investigate possible hydrogen-bonding interactions between Ser-L223 and Q_B and/or Q_B^-, we applied the technique of isotope-edited FTIR difference spectroscopy to the Ser-L223→Ala mutant RC. Upon removing the potential hydrogen bond, perturbations of the carbonyl vibration frequencies should reflect the magnitude of the hydrogen-bonding interaction. The Ser-L223→Ala mutant RC was reconstituted with site-specific ^{13}C-labeled ubiquinone. In the present study, a comparison of the isotope-edited IR fingerprint spectra obtained on the Ser-L223→Ala mutant with those previously reported for wild-type (*31*, *33*) and several mutant RCs from *Rb. sphaeroides* (*34*−*36*) is presented, and the implications are discussed.

EXPERIMENTAL PROCEDURES

The construction of the Ser-L223→Ala site-directed mutant and the isolation of purified RCs are described in ref *11*. A detailed description of the preparation of RC samples for FTIR experiments is given in refs *29*, *31*, and *38*. RC samples in 90 mM Tris buffer pH 7 contained an excess of ubiquinone (Q_6 or Q_3). Q_6 was purchased from Sigma. The synthesis of Q_3 selectively labeled with ^{13}C at the 1- or the 4-position has been reported previously (*39*). The isotopic enrichment of the labeled quinones was better than 99% (*39*).

Steady-state light-induced FTIR difference spectra of the Q_B to Q_B^- transition in native and mutant RCs were recorded at 15 °C with a Nicolet 60SX spectrometer, as described in refs *29*, *31*, and *38*. The Q_B^- state was generated by excitation with a single turnover saturating flash (Nd:YAG laser, 7 ns, 530 nm). The IR sample contains mediators and redox buffer to allow rapid reduction of the photooxidized primary electron donor, therefore eliminating the contributions from P and P^+ species (*29*, *31*, *38*). Difference Q_B^-/Q_B spectra were calculated from each 128 scans (acquisition time: 23 s) recorded before and after laser flash excitation. For a given sample, these measurements were repeated over ∼30 h.

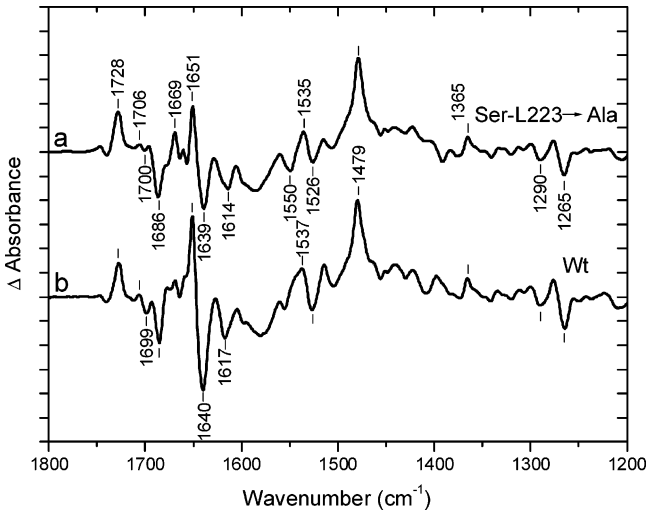

FIGURE 2: Light-induced Q_B^-/Q_B FTIR difference spectra of (a) Ser-L223→Ala mutant and (b) wild-type (Wt) RCs from *Rb. sphaeroides* reconstituted with unlabeled Q_6, pH 7, 15 °C. About 100 000 interferograms were averaged. The frequency of the IR bands is given with an accuracy of ±1 cm^{-1}. For the accuracy of the band intensities, variations are within the thickness of the depicted traces. Spectral resolution was 4 cm^{-1}. Each division on the vertical scale corresponds to 10^{-4} absorbance unit.

RESULTS

Comparison of Q_B^-/Q_B FTIR Spectra of Native RCs and of the Ser-L223→Ala Mutant. Figure 2 shows the Q_B^-/Q_B light-induced FTIR difference spectra of native and Ala-L223 mutant RCs reconstituted with unlabeled Q_6. The Q_B^-/Q_B spectrum of the Ser-L223→Ala mutant (Figure 2a) displays an overall similar shape compared to that of native RCs (Figure 2b). It shows the main characteristic bands of the appearing Q_B^- state at 1728, 1651, 1535, 1479, and 1365 cm^{-1}, and of the disappearing Q_B state at 1686, 1639, 1614, 1526, 1290, and 1265 cm^{-1} (*29*, *31*, *38*). The main difference concerns a decreased amplitude of the differential signal at 1651/1639 cm^{-1} compared to the one observed at 1651/1640 cm^{-1} in native RCs: this latter signal has been assigned in part to protein changes (amide I: 80% peptide C═O stretching) (*29*). In native RCs (Figure 2b), the two carbonyls from the neutral quinone Q_B also contribute at 1641 cm^{-1} (*31*, *32*).

Other differences between native and Ser-L223→Ala RCs (Figure 2) are observed in the amplitude/ratio of several bands or differential signals, e.g., at 1706/1700 cm^{-1} where the amplitude of the signal in the mutant is about one-third of that seen at 1706/1698 cm^{-1} in the native RC, at 1686 cm^{-1} (where the signal is broader in the mutant with a clear shoulder at ∼1677 cm^{-1}), in the 1669−1657 cm^{-1} range, and at 1550/1535/1526 cm^{-1} (amide II: 60% peptide NH bending and 40% CN stretching). It therefore appears that the amplitude of the backbone signals in both the amide I

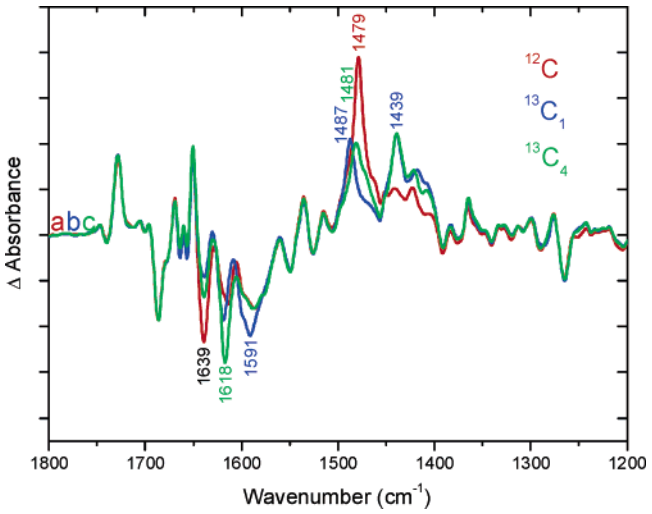

FIGURE 3: Light-induced Q_B^-/Q_B FTIR difference spectra at pH 7, 15 °C of Ser-L223→Ala mutant RCs reconstituted with unlabeled Q_3 (a, red), $^{13}C_1$-labeled Q_3 (b, blue), and $^{13}C_4$-labeled Q_3 (c, green). About 70 000 interferograms were averaged. Each division on the vertical scale corresponds to 10^{-4} absorbance unit.

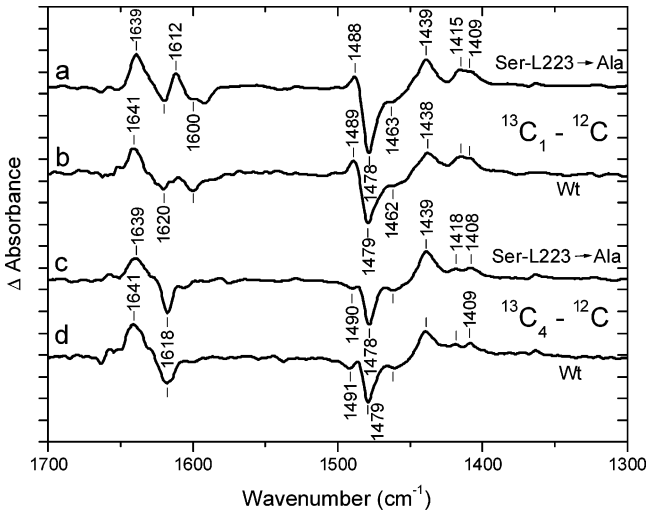

FIGURE 4: Comparison of isotope-edited IR fingerprint spectra (isotopically labeled-minus-unlabeled) obtained for $^{13}C_1$-labeling (a, Ser-L223→Ala; b, native RCs) and $^{13}C_4$-labeling (c, Ser-L223→Ala; d, native RCs). Each division on the vertical scale corresponds to 10^{-4} absorbance unit.

(at 1651/1639 cm^{-1}) and amide II (1550/1535/1526 cm^{-1}) regions is significantly decreased in the Q_B^-/Q_B spectrum of the Ala-L223 RC (Figure 1a). A local distortion of the secondary structure, e.g., a small change of orientation of the Ala peptide group in the mutant compared to that of Ser in the native RCs, or a different coupling of the amide oscillators contributing to the 1651/1639 and 1550/1535/1526 cm^{-1} signals, could account for the changes observed in the Ser-L223→Ala mutant. Alternatively, a direct contribution from the Ser peptide group at 1651/1640 and 1537/1526 cm^{-1} in the Q_B^-/Q_B spectrum of the native RC can be considered.

Similarly to native RCs, the positive signal observed at 1728 cm^{-1} in the Ala-L223 mutant is sensitive to $^1H/^2H$ isotope exchange and is downshifted to 1717 cm^{-1} in ^2H_2O (not shown). The disappearance of this ^2H_2O sensitive signal in the mutant Glu-L212→Gln led to its assignment to substoichiometric proton uptake by Glu-L212 in native RCs upon Q_B reduction (*29*, *40*). The Ser-L223→Ala mutation has no significant effect on the frequency/amplitude of the 1728 cm^{-1} signal (Figure 2a). Thus, Glu-L212 becomes protonated also in the Ser-L223→Ala mutant upon electron transfer to Q_B (*29*, *40*). This result contrasts the computations on the protonation pattern of Glu-L212 in this mutant that indicate that Glu-L212 remains fully ionized in all Q_A and Q_B redox states (*9*).

FTIR changes observed in the Q_B^-/Q_B spectrum of the Ser-L223→Ala mutant (Figure 2a) can be related to different responses of the protein upon semiquinone formation in native and mutant RCs and/or to different interactions of the quinone in the mutant. Only the identification of the IR fingerprint of Q_B and Q_B^- for the Ser-L223→Ala mutant using RCs reconstituted with isotopically labeled ubiquinone can provide an unambiguous assignment of the Q_B and Q_B^- modes with respect to those of the protein.

Q_B and Q_B^- IR Fingerprints of the Ser-L223→Ala Mutant: Study of RCs Reconstituted with Site-Specific ^{13}C-Labeled Ubiquinone. Interactions of Q_B and Q_B^- with the protein in the Ala-L223 mutant RCs were investigated by using specifically labeled Q_3 to reconstitute the Q_B site. Figure 3a−c shows the Q_B^-/Q_B spectra of Ala-L223 RCs reconstituted with unlabeled Q_3, $^{13}C_1$-labeled Q_3, and $^{13}C_4$-labeled Q_3, respectively. In these spectra, several regions, i.e., between 1800 and 1650 cm^{-1}, 1575 and 1500 cm^{-1}, and 1400 and 1200 cm^{-1}, are unaffected by the quinone labeling: these features arise mostly from protein vibrations and from modes of the quinone (methyl, methoxy, and isoprenoid chain) that are essentially insensitive to the labeling of the carbonyl groups. On the other hand, changes are observed in the 1650−1575 and 1500−1400 cm^{-1} regions upon quinone labeling. In both $^{13}C_1$- and $^{13}C_4$-Q_B^-/Q_B spectra (Figure 3b,c), the amplitude of the negative signal at 1639 cm^{-1} is decreased while a large negative signal is observed at ∼1618 cm^{-1}. Furthermore, comparable isotopic effects for $^{13}C_1$- and $^{13}C_4$-labeling occur in the 1500−1400 cm^{-1} spectral range, with large positive bands appearing at 1487 and 1439 cm^{-1} upon $^{13}C_1$-labeling, and at 1481 and 1439 cm^{-1} upon $^{13}C_4$-labeling.

These effects are better visualized in the double-difference spectra (Figure 4a,c) calculated from the individual Q_B^-/Q_B spectra recorded with RCs reconstituted with isotopically labeled and unlabeled Q_3 (^{13}C-minus-^{12}C). In such double-difference spectra, isotope-sensitive vibrations from the quinone itself can be separated from those of the protein that are expected to cancel. The corresponding double-difference spectra $^{13}C_1$-minus-^{12}C and $^{13}C_4$-minus-^{12}C labeling are also displayed for native RCs (*31*) in Figure 4b and Figure 4d, respectively. Figure 4 shows that the IR fingerprint spectra corresponding to the Ala-L223 mutant are highly comparable to those previously obtained for native RCs (*31*−*33*), for both $^{13}C_1$- and $^{13}C_4$-labeling. In these IR fingerprint spectra, the IR bands of the neutral unlabeled quinone (1660−1600 cm^{-1}) appear with a positive sign while the downshifted bands of the labeled quinone exhibit a negative sign. The semiquinone bands in the 1500−1400 cm^{-1} range exhibit a reverse behavior. Such double-difference spectra for $^{13}C_1$- and $^{13}C_4$-labeling represent highly sensitive fingerprints for the interactions of the quinone and semiquinone in their respective protein binding site (*31*).

The IR fingerprint pattern of neutral Q_B (positive bands in the 1660−1600 cm^{-1} region, Figure 4) is essentially the

same in the Ser-L223→Ala mutant as in the native RC. The C═O modes at 1639−1641 cm^{-1} are downshifted to 1620 cm^{-1} upon $^{13}C_1$-labeling (Figure 4a) and to 1618 cm^{-1} upon $^{13}C_4$-labeling (Figure 4c). It therefore appears that both carbonyls of neutral Q_B absorb at nearly the same frequency in the mutant and native RC; the C═O band is downshifted by 2 cm^{-1} in the mutant compared to that observed at 1641 cm^{-1} for native RCs (*31*−*33*). Similarly to native RCs, the C═C modes for the mutant show a shift of the C═C band at 1612 cm^{-1} upon $^{13}C_1$-labeling (Figure 4a) but no effect upon $^{13}C_4$-labeling (Figure 4c), indicating an inequivalence of the C═C modes of neutral Q_B involving the C_1 and C_4 atoms (*31*−*33*).

The IR fingerprint pattern of the semiquinone modes (1500−1400 cm^{-1} region, Figure 4) in the Ser-L223→Ala mutant RCs is also very similar to that of native RCs (*31*−*33*). Both double-difference spectra for $^{13}C_1$ and $^{13}C_4$ labels show a main negative band at 1478 cm^{-1} that is downshifted to 1439 cm^{-1} (positive sign). Consequently, the 1478 cm^{-1} band in the Ala-L223 mutant is attributed to the two C•••O modes coupled to C•••C modes of the semiquinone (*31*). In addition, the small shoulder which is observed at ∼1488 cm^{-1} on the main 1478 cm^{-1} peak of both mutant and native RC spectra (Figure 4) has been tentatively assigned to C•••C modes (*31*). Moreover, this shoulder exhibits a different behavior upon selective $^{13}C_1$- (positive signal at 1488 cm^{-1}) or $^{13}C_4$- (negative signal at ∼1490 cm^{-1}) labeling. This reveals an inequivalence of the C•••C modes of the semiquinone involving the C_1 and C_4 atoms, as described above for the C═C modes of neutral Q_B.

DISCUSSION

IR and Raman spectroscopies have long been used to detect formation or breaking of hydrogen bonds to carbonyl groups. More generally, the frequency of a carbonyl mode is a probe of local electrostatic fields, such as those created by a dipolar hydrogen bond. In the case of bacterial and plant photosystems, vibrational spectroscopy appears to be particularly well-suited to determine the hydrogen bonding or the interaction state of carbonyl groups of cofactors such as chlorophylls (*41*) and quinones (*42*), both in situ and in vitro. More specifically, for *Rb. sphaeroides* RCs, hydrogen bonding to the 9-keto carbonyl of each bacteriochlorophyll half P_A and P_B of the primary electron donor has been observed in the mutant RCs Leu-M160→His and Leu-L131→His, respectively (*43*−*45*). The formation of these hydrogen bonds results in ∼20−30 cm^{-1} frequency downshifts of the 9-keto C═O modes of P_A or P_B. The removal or creation of hydrogen bonds to the 2a-acetyl groups of P_A and P_B has also been observed by FT Raman spectroscopy (*45*). Hydrogen bonding to the 9-keto carbonyl of the (bacterio)pheophytin electron acceptor (H_A) in RCs from *Rb. sphaeroides* (*46*−*48*) and *Bl. viridis* (*47*, *49*) and in D_1D_2 particles (*50*, *51*) has been also inferred from Raman and FTIR with frequency downshifts of ∼20−30 cm^{-1} with respect to the isolated (bacterio)pheophytin *a* model compound. Similarly, hydrogen bonding to the 9-keto and 10a-ester carbonyls of the chlorophylls of P700 in the photosystem I has been recently demonstrated (*52*−*54*). For the bacterial RC, the FTIR data on the photooxidized primary donor and the photoreduced bacteriopheophytin H_A^- are in good agreement with the results from ENDOR measurements (*55*, *56*).

For the quinone carbonyls in native RCs from *Rb. sphaeroides*, asymmetric hydrogen bonds for Q_A (at 1660 and 1601 cm^{-1}) and symmetric hydrogen bonds for Q_B (at 1641 cm^{-1}) have been inferred from IR isotope-edited fingerprint spectra of RCs reconstituted with specifically labeled ubiquinone (*31*, *32*, *42*, *57*, 58). For the semiquinone Q_A^-, the IR fingerprint spectra in native RCs display very different patterns upon $^{13}C_1$- or $^{13}C_4$-labeling (*57*, *58*), indicative of asymmetrical interactions of Q_A^- with the protein. In native RCs, the behavior of the anion Q_A^- modes is thus very different from that observed for Q_B^- (*31*−*33*). Therefore, for Q_A^- and Q_B^-, the FTIR data are in good agreement with ENDOR and EPR measurements (*59*, *60*, *61* and references therein) showing asymmetric interactions of Q_A^- with the protein and more symmetrical interactions of Q_B^- with weaker hydrogen bonds to its binding site.

Bonding Interactions of Q_B and Q_B^- Carbonyls with the Protein in the Ser-L223→Ala Mutant. The isotope-edited IR spectra of the Ser-L223→Ala mutant RCs reconstituted with selectively labeled Q_3 display a unique C═O band at 1639 cm^{-1} (Figure 4a,c). These data demonstrate that both carbonyls of neutral Q_B contribute equally at 1639 cm^{-1} and that each carbonyl of Q_B is engaged in comparable interactions with the protein. The frequency downshift of the 1639 cm^{-1} band with respect to isolated ubiquinone (1664−1650 cm^{-1}, see refs *57* and *62*) indicates moderate hydrogen bonding of Q_B to the protein binding site. Such a symmetrical bonding pattern for the two carbonyls of Q_B fits the description of the proximal binding site for neutral Q_B in the Ser-L223→Ala RC, as previously demonstrated for native RCs (*31*, *33*) and a number of mutant RCs at the Q_B site (*34*−*36*). The 2 cm^{-1} frequency downshift that is observed for the carbonyl band in the mutant compared to native RCs (Figure 4) could result from local changes of the dielectric constant upon removal of the Ser hydroxyl group. Similarly, the absence of splitting of the 1478 cm^{-1} band and its comparable frequency downshift upon either $^{13}C_1$- or $^{13}C_4$-labeling favor equivalent hydrogen-bonding interactions of the two carbonyls of Q_B^- to the protein in the Ser-L223→Ala RC. Moreover, the frequency/intensity of the modes associated with the semiquinone formation are identical (±1 cm^{-1}) in native RCs and in the Ala-L223 mutant, indicative of highly equivalent interactions of the Q_B^- anion with the protein in both RCs.

The present study of the Ser-L223→Ala mutant thus shows that the removal of the hydroxyl side chain in the Ala-L223 mutant has essentially no effect on the quinone and semiquinone modes of Q_B. Assuming that in native RCs the C_1 carbonyl of the quinone interacts with the hydroxyl of Ser-L223 in Q_B and/or Q_B^- states, as proposed from some X-ray data (*4*, *16*−*18*, *23*), electrostatic calculations (*8*−*10*), and recent ENDOR experiments at 77 K (*26*, *27*), we would have expected to observe changes in the IR fingerprint pattern of the quinone/semiquinone of the Ser-L223→Ala mutant. More precisely, the loss of one of the three branched hydrogen bonds (with the peptide NH of Ile-L224 and Gly-L225 and the hydroxyl of Ser-L223) to the C_1 carbonyl oxygen of Q_B in the mutant would be expected to increase the observed vibration frequencies, assuming that the strength of the two other branched hydrogen bonds remains unchanged. Instead,

the C═O band of Q_B and the C•••O band of Q_B^- are decreased by 1−2 cm^{-1} in the mutant compared to the bands observed at 1641 and 1479 cm^{-1}, respectively, in the native RC (*31*, *32*). These shifts correspond to a difference in binding energy of ∼0.1−0.3 kcal·mol^{-1} according to the Badger and Bauer rule that relates the frequency shifts of C═O stretching vibrations to the energies of hydrogen bonds (*63*). This small magnitude of the frequency shifts shows that there is essentially no net change in the interaction of the carbonyl oxygen atoms of Q_B and Q_B^- with the protein upon removal of the Ser-L223 hydroxyl group. Thus, for both native and mutant RCs, Q_B^- remains strongly bound to the protein, presumably due to the strong hydrogen bond interactions with the backbone NH groups of Ile-L224 and Gly-L225.

While the frequency/intensity of the modes associated with the semiquinone formation are essentially identical (±1 cm^{-1}) in the native and Ser-L223→Ala mutant RCs, perturbations of the semiquinone modes have previously been observed for several mutant RCs with amino acid substitutions close to Q_B. Such changes are most striking in RCs that contain mutations of Asp-L213 (*29*, *36*, *64*) or of Pro-L209 (*34*, *35*) sites. When the isotope-edited IR spectra of these mutant RCs have been obtained (*34*−*36*), they differ notably in the semiquinone range for the C_1- and the C_4-labeling of ubiquinone. Importantly, they display a large splitting of the anion band for C_4-labeling compared to the main single anion band in native RCs (*31*). Indeed, X-ray structures of RCs with mutations at L213 or L209 sites (*65*, *66*) show that the mutations cause a number of local structural changes around the quinone site involving displacements of side chains and/or backbone and possible realignment of water molecules. Therefore, the electrostatic interactions near the quinone are expected to be different in these mutants compared to native RCs, and consequently, it should have an effect on the electronic structure and/or the hydrogen-bonding pattern of the anion, and thus on the frequency/intensity of the semiquinone bands in the spectra of the mutant RCs.[2]

Model of the Interaction between Ser-L223 and Q_B or Q_B^- and the Surrounding Protein. The interaction between Ser-L223 and Q_B or Q_B^- can be inferred from the effect of the Ser-L223→Ala mutation on the carbonyl vibration frequency. The FTIR spectra of the specifically ^{13}C-labeled quinones show that the vibration frequencies of the C_1 and C_4 carbonyls are the same in the mutant and the native RC (Figure 4). This indicates that Ser-L223 does not have a significant interaction with either Q_B or Q_B^- in the native RC. The simplest model to explain the FTIR data is that the Ser-L223 hydroxyl group forms a more stable hydrogen bond with another group than with the C_1 carbonyl group of the quinone. The most likely candidate would be Asp-L213, which is located within hydrogen-bonding proximity (see *e.g.* ref *4*) and has been calculated to form a stable hydrogen bond when Asp-L213 is ionized (*8*−*10*). These results imply that Asp-L213 retains some ionized character in the Q_B^- state as has been proposed from previous FTIR results which do not show protonated carboxylic bands associated with Asp-L213 (*29*, *30*).

The proposed scenario could arise due to the *unique* design of the Q_B pocket. The quinone carbonyl with which Ser-L223 might transiently interact has the unusual feature of possibly forming a multiple hydrogen bond with three different groups, the peptide NH of Ile-L224 and of Gly-L225 and the Ser-L223 hydroxyl group (Figure 1). This allows different groups to provide hydrogen bonds for distinct functions. For example, hydrogen bonds from the backbone are important for Q_B binding and provide stability to the radical Q_B^- state, whereas the Ser-L223 hydroxyl group is allowed to form hydrogen bonds to both Asp-L213 and Q_B^- facilitating proton transfer along the proton-transfer chain (see below).

Role of Ser-L223 in the Gating Step. The kinetic gate that limits the first electron transfer occurs at a step that involves the uphill formation of an intermediate state $(Q_A^-Q_B)^*$ (see eq 1). Transfer then proceeds downhill to the $Q_AQ_B^-$ state (*2*). The FTIR results show that Ser-L223 does not have a significant interaction with either Q_B or Q_B^-. Thus, hydrogen bonding between Q_B and Ser-L223 cannot be a major factor in determining the energy of the intermediate state. This is consistent with the nearly unaltered reaction kinetics observed in the mutant RCs for the first electron transfer (*12*). Although several calculations propose that the Ser-L223 hydroxyl proton flip between Asp-L213 and Q_B upon its reduction (*9*, *10*), the FTIR results indicate that the hydrogen bond, if formed, is too weak to be *by itself* the conformational gate associated with the first electron transfer to Q_B (*2*). Other interactions of larger magnitude are likely involved in the conformational gate.

Role of Ser-L223 in Proton Transfer to Q_B^- and Binding of Q_B^-. The importance of Ser-L223 in proton transfer to reduced Q_B has been demonstrated by the 10^3-fold decrease in the observed rate of $k_{AB}^{(2)}$ (see eq 2) in the Ser-L223→Ala mutant RC compared to the native RC (*12*). In addition, computational work suggests that a hydrogen bond is formed between the hydroxyl group of the Ser and Q_B^- upon its formation (*8*−*10*). Preliminary ENDOR experiments at 77 K are consistent with that proposal (*26*, *27*). The FTIR results presented here show that the Ser hydroxyl group does not form a strong hydrogen bond to either Q_B or Q_B^-. All of these results can be rationalized with a model in which Ser-L223 can alternate hydrogen bonds with Asp-L213 and Q_B^-.

A model consistent with these results is that the Ser-L223 OH group is predominately hydrogen bonded to Asp-L213.[3] This does not exclude that a small fraction of the Ser OH

[2] Similarly, the small differences observed in the semiquinone IR fingerprint pattern of *Rb. sphaeroides* and *Bl. viridis* RCs have been related to the few residues lining the binding pocket that differ between the two organisms and that can differently affect the electrostatic environment of the quinone (*31*).

[3] In the proposed model, the Ser-L223 OH group interacts with the ionized Asp-L213. Thus, the Ser-L223 to Ala mutation would be expected to perturb the interactions of Asp-L213 with its neighbors. However, such an effect cannot be assessed since specific carboxylate modes (asymmetric and symmetric COO^- modes at ∼1570 and 1400 cm^{-1}, respectively) have not been assigned for Asp-L213.

[4] A crude estimate of the small fraction of the Ser OH group that can be hydrogen bonded to Q_B^- can be inferred from the analysis of the 1500−1400 cm^{-1} anion region in the calculated double-difference spectrum between Q_B^-/Q_B spectra of mutant and native RCs (not shown). Apart from the shift of the main peak at 1479−1478 cm^{-1}, the double-difference spectrum shows only very small differences around 1465 cm^{-1}, suggesting that at most 5% of Ser OH could be hydrogen bonded to Q_B^-.

groups are hydrogen bonded to Q_B^-.[4] The ability of the Ser OH proton to alternate hydrogen bonds between Asp L213 and Q_B^- is an important property for its role in proton transfer through hydrogen-bonded chains (*67*). There are two steps necessary for proton transfer through a hydrogen-bonded chain via a Grotthuss mechanism (*67*, *68*). The first involves concomitant proton transfer through the hydrogen bonds along the hydrogen-bonded chain (proton-transfer step), and the second involves orientating the hydrogen-bonded network back to the proton-transfer configuration (orientation step). The fluctuation of the Ser-L223 proton from Asp-L213 to Q_B^- (orientation step) creates the hydrogen-bonded chain through which proton transfer from Asp-L213 to Q_B^- can occur via Ser-L233 (proton-transfer step). Thus, for this model of proton transfer the ability of the Ser-L223 OH bond to fluctuate between Asp-L213 and Q_B^- is a key step in the proton transfer to reduced Q_B.

Although the Ser-L223 hydroxyl group can be removed with no significant changes to the FTIR spectra, both the quinone and in particular the semiquinone remain firmly bound and show similar interactions with the protein. These results are also consistent with optical kinetic studies in the Ser-L223→Ala mutant RC that show little changes in the redox potential of Q_B^- as determined from the lifetime of the charge-separated $P^+Q_B^-$ state (*11*, *12*). This is a particular feature of the Q_B site that is likely designed to inhibit the release of the potential damaging semiquinone radical. Thus, the Q_B site has the unique characteristics of binding and stabilizing Q_B^- (with hydrogen bonds from the protein backbone) while at the same time allowing the Ser-L223 hydroxyl group to have the necessary flexibility required for its role in the proton-transfer chain.

ACKNOWLEDGMENT

We thank Claude Boullais and Charles Mioskowski for the synthesis of the labeled quinones.

REFERENCES

1. Okamura, M. Y., Paddock, M. L., Graige, M. S., and Feher, G. (2000) Proton and electron transfer in bacterial reaction centers, *Biochim. Biophys. Acta 1458*, 148−163.
2. Graige, M. S., Feher, G., and Okamura, M. Y. (1998) Conformational gating of the electron transfer reaction $Q_A^-Q_B \rightarrow Q_AQ_B^-$ in bacterial reaction centers of *Rhodobacter sphaeroides* determined by a driving force assay, *Proc. Natl. Acad. Sci. U.S.A. 95*, 11679−11684.
3. Graige, M. S., Paddock, M. L., Bruce, J. M., Feher, G., and Okamura, M. Y. (1996) Mechanism of proton-coupled electron transfer for quinone (Q_B) reduction in reaction centers of *Rb. sphaeroides*, *J. Am. Chem. Soc. 118*, 9005−9016.
4. Stowell, M. H. B., McPhillips, T. M., Rees, D. C., Soltis, S. M., Abresch, E., and Feher, G. (1997) Light-induced structural changes in photosynthetic reaction center: Implications for mechanism of electron-proton transfer, *Science 276*, 812−816.
5. Abresch, E. C., Paddock, M. L., Stowell, M. H. B., McPhillips, T. M., Axelrod, H. L., Soltis, S. M., Rees, D. C., Okamura, M. Y., and Feher, G. (1998) Identification of proton transfer pathways in the X-ray structure of the bacterial reaction center from *Rhodobacter sphaeroides*, *Photosynth. Res. 55*, 119−125.
6. Paddock, M. L., Feher, G., and Okamura, M. Y. (2003) Proton transfer pathways and mechanism in bacterial reaction centers, *FEBS Lett. 555*, 45−50.
7. Wraight, C. A. (2004) Proton and electron transfer in the acceptor quinone complex of photosynthetic reaction centers from *Rhodobacter sphaeroides*, *Front. Biosci. 9*, 309−337.
8. Alexov, E. G., and Gunner, M. R. (1999) Calculated protein and proton motions coupled to electron transfer: Electron transfer from Q_A^- to Q_B in bacterial photosynthetic reaction centers, *Biochemistry 38*, 8253−8270.
9. Ishikita, H., and Knapp, E.-W. (2004) Variation of Ser-L223 hydrogen bonding with the Q_B redox state in reaction centers from *Rhodobacter sphaeroides*, *J. Am. Chem. Soc. 126*, 8059−8064.
10. Zhu, Z., and Gunner, M. R. (2005) Energetics of quinone-dependent electron and proton transfers in *Rhodobacter sphaeroides* photosynthetic reaction centers, *Biochemistry 44*, 82−96.
11. Paddock, M. L., McPherson, P. H., Feher, G., and Okamura, M. Y. (1990) Pathway of proton transfer in bacterial reaction centers: Replacement of serine-L223 by alanine inhibits electron and proton transfers associated with reduction of quinone to hydroquinone, *Proc. Natl. Acad. Sci. U.S.A. 87*, 6803−6807.
12. Paddock, M. L., Feher, G., and Okamura, M. Y. (1995) Pathway of proton transfer in bacterial reaction centers: Further investigations on the role of Ser-L223 studied by site-directed mutagenesis, *Biochemistry 34*, 15742−15750.
13. Paddock, M. L., Rongey, S. H., Abresch, E. C., Feher, G., and Okamura, M. Y. (1988) Reaction centers from three herbicide-resistant mutants of *Rhodobacter sphaeroides* 2.4.1: Sequence analysis and preliminary characterization, *Photosynth. Res. 17*, 75−96.
14. Leibl, W., Sinning, I., Ewald, G., Michel, H., and Breton, J. (1993) Evidence that Ser-L223 is involved in the proton transfer pathway to Q_B in the photosynthetic reaction center of *Rhodopseudomonas viridis*, *Biochemistry 32*, 1958−1964.
15. Deisenhofer, J., and Michel, H. (1989) The photosynthetic reaction centre from the purple bacterium *Rhodopseudomonas viridis*, *EMBO J. 8*, 2149−2170.
16. Allen, J. P., Feher, G., Yeates, T. O., Komiya, H., and Rees, D. C. (1988) Structure of the reaction center from *Rhodobacter sphaeroides* R-26: Protein-cofactor (quinones and Fe^{2+}) interactions, *Proc. Natl. Acad. Sci. U.S.A. 85*, 8487−8491.
17. El-Kabbani, O., Chang, C.-H., Tiede, D., Norris, J., and Schiffer, M. (1991) Comparison of reaction centers from *Rhodobacter sphaeroides* and *Rhodopseudomonas viridis*: Overall architecture and protein-pigment interactions, *Biochemistry 30*, 5361−5369.
18. Chirino, A. J., Lous, E. J., Huber, M., Allen, J. P., Schenck, C. C., Paddock, M. L., Feher, G., and Rees, D. C. (1994) Crystallographic analyses of site-directed mutants of the photosynthetic reaction center from *Rhodobacter sphaeroides*, *Biochemistry 33*, 4584−4593.
19. Ermler, U., Fritzsch, G., Buchanan, S. K., and Michel, H. (1994) Structure of the photosynthetic reaction centre from *Rhodobacter sphaeroides* at 2.65 Å resolution: Cofactors and protein−cofactor interactions, *Structure 2*, 925−936.
20. Arnoux, B., and Reiss-Husson, F. (1996) Pigment-protein interactions in *Rhodobacter sphaeroides* Y photochemical reaction center; Comparison with other reaction center structures, *Eur. Biophys. J. 24*, 233−242.
21. Lancaster, C. R. D., Ermler, U., and Michel, H. (1995) The structures of photosynthetic reaction centres from purple bacteria as revealed by X-ray crystallography, in *Anoxygenic Photosynthetic Bacteria* (Blankenship, R. E., Madigan, M. T., and Bauer, C. E., Eds.), pp 503−526, Kluwer Academic Publishers, Dordrecht, The Netherlands.
22. Fritzsch, G., Koepke, J., Diem, R., Kuglstatter, A., and Baciou, L. (2002) Charge separation induces conformational changes in the photosynthetic reaction centre of purple bacteria, *Acta Crystallogr. D 58*, 1660−1663.
23. McAuley, K. E., Fyfe, P. K., Ridge, J. P., Cogdell, R. J., Isaacs, N. W., and Jones, M. (2000) Ubiquinone binding, ubiquinone exclusion, and detailed cofactor conformation in a mutant bacterial reaction center, *Biochemistry 39*, 15032−15043.
24. Paddock, M. L., Chang, C., Xu, Q., Abresch, E. C., Axelrod, H. L., Feher, G., and Okamura, M. Y. (2005) Quinone (Q_B) reduction by B-branch electron transfer in mutant bacterial reaction centers from *Rhodobacter sphaeroides*: Quantum efficiency and X-ray structure, *Biochemistry 44*, 6920−6928.
25. Pokkuluri, P. R., Laible, P. D., Crawford, A. E., Mayfield, J. F., Yousef, M. A., Ginell, S. L., Hanson, D. K., and Schiffer, M. (2004) Temperature and cryoprotectant influence secondary quinone binding position in bacterial reaction centers, *FEBS Lett. 570*, 171−174.
26. Paddock, M. L., Flores, M., Isaacson, R., Chang, C., Abresch, E. C., Selvaduray, P., Feher, G., and Okamura, M. Y. (2005) $Q_B^{-\bullet}$ formed by B-branch electron transfer in reaction centers from *Rhodobacter sphaeroides*, in *Photosynthesis: Fundamental As-*

pects to Global Perspectives (van der Est, A., and Bruce, D., Eds.), pp. 207−209, Alliance Communications Group, Lawrence, KA.
27. Paddock, M. L., Flores, M., Isaacson, R. A., Chang, C., Selvaduray, P., Feher, G., and Okamura, M. Y. (2005) Hydrogen bond reorientation upon Q_B reduction revealed by ENDOR spectroscopy in reaction centers from *Rhodobacter sphaeroides*, *Biophys. J. 88*, A204.
28. Bibikov, S. I., Bloch, D. A., Cherepanov, A., Oesterhelt, D., and Semenov, A. Yu. (1994) Flash-induced electrogenic reactions in the SA(L223) reaction center mutant in *Rhodobacter sphaeroides* chromatophores, *FEBS Lett. 341*, 10−14.
29. Nabedryk, E., Breton, J., Hienerwadel, R., Fogel, C., Mäntele, W., Paddock, M. L., and Okamura, M. Y. (1995) Fourier transform infrared difference spectroscopy of secondary quinone acceptor photoreduction in proton transfer mutants of *Rhodobacter sphaeroides*, *Biochemistry 34*, 14722−14732.
30. Nabedryk, E., Breton, J., Hienerwadel, R., Fogel, C., Mäntele, W., Paddock, M. L., and Okamura, M. Y. (1995) FTIR spectroscopy of Q_B photoreduction in *Rhodobacter sphaeroides* reaction centers: Effects of site-directed replacements at Glu L212, Asp L213, Asp L210, and of $^1H/^2H$ exchange, in *Photosynthesis: from Light to Biosphere* (Mathis, P., Ed.) Vol. I, pp 875−878, Kluwer Academic Publishers, Dordrecht, The Netherlands.
31. Breton, J., Boullais, C., Berger, G., Mioskowski, C., and Nabedryk, E. (1995) Binding sites of quinones in photosynthetic bacterial reaction centers investigated by light-induced FTIR difference spectroscopy: Symmetry of the carbonyl interactions and close equivalence of the Q_B vibrations in *Rhodobacter sphaeroides* and *Rhodopseudomonas viridis* probed by isotope labeling, *Biochemistry 34*, 11606−11616.
32. Brudler, R., de Groot, H. J. M., van Liemt, W. B. S., Gast, P., Hoff, A. J., Lugtenburg, J., and Gerwert, K. (1995) FTIR spectroscopy shows weak symmetric hydrogen bonding of the Q_B carbonyl groups in *Rhodobacter sphaeroides* R26 reaction centers, *FEBS Lett. 370*, 88−92.
33. Breton, J. (2004) Absence of large-scale displacement of quinone Q_B in bacterial photosynthetic reaction centers, *Biochemistry 43*, 3318−3326.
34. Breton, J., Boullais, C., Mioskowski, C., Sebban, P., Baciou, L., and Nabedryk, E. (2002) Vibrational spectroscopy favors a unique Q_B binding site at the proximal position in wild-type reaction centers and in the Pro-L209 → Tyr mutant from *Rhodobacter sphaeroides*, *Biochemistry 41*, 12921−12927.
35. Nabedryk, E., Breton, J., Sebban, P., and Baciou, L. (2003) Quinone (Q_B) binding site and protein structural changes in photosynthetic reaction center mutants at Pro-L209 revealed by vibrational spectroscopy, *Biochemistry 42*, 5819−5827.
36. Breton, J., Wakeham, M. C., Fyfe, P. K., Jones, M. R., and Nabedryk, E. (2004) Characterization of the bonding interactions of Q_B upon photoreduction via A-branch or B-branch electron transfer in mutant reaction centers from *Rhodobacter sphaeroides*, *Biochim. Biophys. Acta 1656*, 127−138.
37. Breton, J., Nabedryk, E., Boullais, C., Mioskowski, C., Paddock, M. L., Feher, G., and Okamura, M. Y. (1997) Interaction of Q_B and Q_B^- with the protein in native and Ser-L223→Ala *Rb. sphaeroides* reaction centers probed by light-induced FTIR difference spectroscopy, *Biophys. J. 72*, A7.
38. Breton, J., Berthomieu, C., Thibodeau, D. L., and Nabedryk, E. (1991) Probing the secondary quinone environment (Q_B) in photosynthetic bacterial reaction centers by light-induced FTIR difference spectroscopy, *FEBS Lett. 288*, 109−113.
39. Boullais, C., Nabedryk, E., Burie, J.-R., Nonella, M., Mioskowski, C., and Breton, J. (1998) Site-specific isotope-labeling demonstrates a large mesomeric resonance effect of the methoxy groups on the carbonyl frequencies in ubiquinones, *Photosynth. Res. 55*, 247−252.
40. Nabedryk, E., Breton, J., Okamura, M. Y., and Paddock, M. L. (2001) Simultaneous replacement of Asp-L210 and Asp-M17 with Asn increases proton uptake by Glu-L212 upon first electron transfer to Q_B in reaction centers from *Rhodobacter sphaeroides*, *Biochemistry 40*, 13826−13832.
41. Lutz, M., and Mäntele, W. (1991) Vibrational spectroscopy of chlorophylls in *The Chlorophylls* (Scheer, H., Ed.) pp 855−902, CRC Press, Boca Raton, FL.
42. Breton, J., and Nabedryk, E., (1996) Protein-interactions in the bacterial photosynthetic reaction center: Light-induced FTIR difference spectroscopy of the quinone vibrations, *Biochim. Biophys. Acta 1275*, 84−90.
43. Nabedryk, E., Allen, J. P., Taguchi, A. K. W., Williams, J. C., Woodbury, N. W., and Breton, J. (1993) Fourier transform infrared study of the primary electron donor in chromatophores of *Rhodobacter sphaeroides* with reaction centers genetically modified at residues M160 and L131, *Biochemistry 32*, 13879−13885.
44. Mattioli, T. A., Williams, J. C., Allen, J. P., and Robert B. (1994) Changes in primary donor hydrogen-bonding interactions in mutant reaction centers from *Rhodobacter sphaeroides*: Identification of the vibrational frequencies of all the conjugated carbonyl groups, *Biochemistry 33*, 1636−1643.
45. Mattioli, T. A., Lin, X., Allen, J. P., and Williams, J. C. (1995) Correlation between multiple hydrogen bonding and alteration of the oxidation potential of the bacteriochlorophyll dimer of reaction centers from *Rhodobacter sphaeroides*, *Biochemistry 34*, 6142−6152.
46. Robert, B. (1990) Resonance Raman studies of bacterial reaction centers, *Biochim. Biophys. Acta 1017*, 99−111.
47. Nabedryk, E., Andrianambinintsoa, S., Dejonghe, D., and Breton, J. (1995) FTIR spectroscopy of the photoreduction of the bacteriopheophytin electron acceptor in reaction centers of *Rb. sphaeroides* and *Rps. viridis*, *Chem. Phys. 194*, 371−378.
48. Palaniappan, V., and Bocian, D. F. (1995) Resonance Raman spectroscopic evidence for dielectric asymmetry in bacterial photosynthetic reaction centers, *J. Am. Chem. Soc. 117*, 3647−3648.
49. Breton, J., Bibikova, M., Oesterhelt, D., and Breton, J. (1999) Conformational heterogeneity of the bacteriopheophytin electron acceptor H_A in reaction centers from *Rhodopseudomonas viridis* revealed by Fourier transform infrared spectroscopy and site-directed mutagenesis, *Biochemistry 38*, 11541−11552.
50. Moenne-Loccoz, P., Robert, B., and Lutz, M. (1989) A resonance Raman characterization of the primary electron acceptor in photosystem II, *Biochemistry 28*, 3641−3645.
51. Nabedryk, E., Andrianambinintsoa, S., Berger, G., Leonhard, M., Mäntele, W., and Breton, J. (1990) Characterization of bonding interactions of the intermediary electron acceptor in the reaction center of photosystem II by FTIR spectroscopy, *Biochim. Biophys. Acta 1016*, 49−54.
52. Pantelidou, M., Chitnis, P. R., and Breton, J. (2004) FTIR spectroscopy of *Synechocystis* 6803 mutants affected on the hydrogen bonds to the carbonyl groups of the PsaA chlorophyll of P700 supports an extensive delocalization of the charge in $P700^+$, *Biochemistry 43*, 8380−8390.
53. Breton, J., Chitnis, P. R., and Pantelidou, M. (2005) Evidence for hydrogen bond formation to the PsaB chlorophyll of P700 in photosystem I mutants of *Synechocystis* sp. PCC 6803, *Biochemistry 44*, 5402−5408.
54. Witt, H., Schlodder, E., Teutloff, C., Niklas, J., Bordignon, E., Carbonera, D., Kohler, S., Labahn, A., and Lubitz, W. (2002) Hydrogen bonding to P700: Site-directed mutagenesis of threonine A739 of photosystem I of *Chlamydomonas reinhardtii*, *Biochemistry 41*, 8557−8569.
55. Rautter, J., Lendzian, F., Schulz, C., Fetsch, A., Kuhn, M., Lin, X., Williams, J. C., Allen, J. P., and Lubitz, W. (1995) ENDOR studies of the primary donor cation radical in mutant reaction centers of *Rhodobacter sphaeroides* with altered hydrogen-bond interactions, *Biochemistry 34*, 8130−8143.
56. Lubitz, W., Bönigk, B., Plato, M., Isaacson, R. A., Okamura, M. Y., and Feher, G. (1990) ENDOR studies of the intermediate electron acceptor radical anion $I^{-\bullet}$ in reaction centers of *Rps. viridis*, in *Current Research in Photosynthesis* (Baltscheffsky, M., Ed.) Vol. I, pp 141−144, Kluwer Academic Publishers, Dordrecht, The Netherlands.
57. Breton, J., Boullais, C., Burie, J.-R., Nabedryk, E., and Mioskowski, C. (1994) Binding sites of quinones in photosynthetic bacterial reaction centers investigated by light-induced FTIR difference spectroscopy: Assignment of the interactions of each carbonyl of Q_A in *Rhodobacter sphaeroides* using site-specific ^{13}C-labeled ubiquinone, *Biochemistry 33*, 14378−14386.
58. Brudler, R., de Groot, H. J. M., van Liemt, W. B. S., Steggerda, W. F., Esmeijer, Gast, P., Hoff, A. J., Lugtenburg, J., and Gerwert, K. (1994) Asymmetric binding of the 1- and 4-C═O groups of Q_A in *Rhodobacter sphaeroides* R26 reaction centers monitored by Fourier transform infra-red spectroscopy using site-specific isotopically labelled ubiquinone-10, *EMBO J. 13*, 5523−5530.
59. Feher, G., Isaacson, R. A., Okamura, M. Y., and Lubitz, W. (1985) ENDOR of semiquinones in RCs from *Rhodopseudomonas sphaeroides*, in *Antennas and Reaction centers of Photosynthetic Bacteria—Structure, Interactions and Dynamics* (Michel-Beyerle,

M. E., Ed.) Springer Series in Chemical Physics, Vol. 42, pp 174−189, Springer, Berlin.

60. van der Brink, J. S., Spoyalov, A. P., Gast, P., van Liemt, W. B. S., Raap, J., Lugtenburg, J., and Hoff, A. J. (1994) Asymmetric binding of the primary quinone acceptor in reaction centers of the photosynthetic bacterium *Rhodobacter sphaeroides* R26, probed with Q-band (35 GHz) EPR spectroscopy, *FEBS Lett. 353*, 273−276.
61. Lubitz, W., and Feher, G. (1999) The primary and secondary acceptors in bacterial photosynthesis. III Characterization of the quinone radicals $Q_A^{-\bullet}$ and $Q_B^{-\bullet}$ by EPR and ENDOR, *Appl. Magn. Reson. 17*, 1−48.
62. Burie, J.-R., Boullais, C., Nonella, M., Mioskowski, C., Nabedryk, E., and Breton, J. (1997) Importance of the conformation of methoxy groups on the vibrational and electrochemical properties of ubiquinones, *J. Phys. Chem. B 101*, 6607−6617.
63. Badger, R. M., and Bauer, S. H. (1937) Spectroscopic studies of the hydrogen bond. II The shift of the O-H vibrational frequency in the formation of the hydrogen bond, *J. Chem. Phys. 5*, 839−851.
64. Nabedryk, E., Breton, J., Okamura, M. Y., and Paddock, M. L. (2004) Identification of a novel protonation pattern for carboxylic acids upon Q_B photoreduction in *Rhodobacter sphaeroides* reaction center mutants at Asp-L213 and Glu-L212 sites, *Biochemistry 43*, 7236−7243.
65. Pokkuluri, P. R., Laible, P. D., Deng, Y.-L., Wong, T. N., Hanson, D. K., and Schiffer, M. (2002) The structure of a mutant photosynthetic reaction center shows unexpected changes in main chain orientations and quinone position, *Biochemistry 41*, 5998−6007.
66. Kuglstatter, A., Ermler, U., Michel, H., Baciou, L., and Fritzsch, G. (2001) X-ray structure analyses of photosynthetic reaction center variants from *Rhodobacter sphaeroides*: Structural changes induced by point mutations at position L209 modulate electron and proton transfer, *Biochemistry 40*, 4253−4260.
67. Nagle, J. F., and Tristram-Nagle, S. (1983) Hydrogen bonded chain mechanisms for proton conduction and proton pumping, *J. Membr. Biol. 74*, 1−14.
68. Eigen, M. (1964). Proton transfer, acid-base catalysis, and enzymatic hydrolysis, *Angew. Chem., Int. Ed. Engl. 3*, 1−72.

BI051328D